AEROSPACE NAVIGATION SYSTEMS

EDITED BY ALEXANDER V. NEBYLOV & JOSEPH WATSON

WILEY

AEROSPACE NAVIGATION SYSTEMS

AEROSPACE NAVIGATION SYSTEMS

Edited by

Alexander V. Nebylov
Joseph Watson

WILEY

This edition first published 2016

First Edition published in 2016

Registered Office
John Wiley & Sons, Ltd, The Atrium, Southern Gate, Chichester, West Sussex, PO19 8SQ, United Kingdom

For details of our global editorial offices, for customer services and for information about how to apply for permission to reuse the copyright material in this book please see our website at www.wiley.com.

Library of Congress Cataloging-in-Publication Data

Names: Nebylov, A. V. (Aleksandr Vladimirovich), editor. | Watson, Joseph, 1931– editor.
Title: Aerospace navigation systems / [edited by] Alexander V. Nebylov, Joseph Watson.
Description: First edition. | Chichester, West Sussex, United Kingdom : John Wiley & Sons Ltd., 2016. | Includes bibliographical references and index.
Identifiers: LCCN 2015047272 (print) | LCCN 2015049979 (ebook) | ISBN 9781119163077 (cloth) | ISBN 9781119163039 (Adobe PDF) | ISBN 9781119163046 (ePub)
Subjects: LCSH: Navigation (Aeronautics) | Aids to air navigation. | Navigation (Astronautics)
Classification: LCC TL586 .A28 2016 (print) | LCC TL586 (ebook) | DDC 629.135/1–dc23
LC record available at http://lccn.loc.gov/2015047272

A catalogue record for this book is available from the British Library.

Set in 10/12pt Times by SPi Global, Pondicherry, India

1 2016

Contents

The Editors

Alexander V. Nebylov graduated with honors as an engineer in Missile Guidance from the Leningrad Institute of Aircraft Instrumentation in 1971. He led many R&D projects in aerospace instrumentation, motion control systems, and avionics, and he is a scientific consultant for various Russian design bureaus and research institutes. He was awarded the Candidate of Science degree in 1974 and the Doctor of Science degree in 1985, both in information processing and control systems, from the State Academy of Aerospace Instrumentation. He achieved the academic rank of full professor in the Higher Attestation Commission of the USSR in 1986.

For the past two decades, Dr. Nebylov has been with the State University of Aerospace Instrumentation in St. Petersburg as Professor and Chairman of Aerospace Devices and Measuring Complexes, and Director of the International Institute for Advanced Aerospace Technologies. He is the author of 15 books and numerous scientific papers and has also been a member of the leadership of the IFAC Aerospace Technical Committee since 2002. He has also been a member of the Presidium of the International Academy of Navigation and Motion Control since 1995. In 2006, the title of Honored Scientist of the Russian Federation was bestowed on Dr. Nebylov.

Joseph Watson is an electrical engineering graduate of the University of Nottingham, England, and the Massachusetts Institute of Technology, where he held a King George VI Memorial Fellowship. A fellow of the IET, senior member of the IEEE, and a member of Sigma Xi (the Scientific Research Society of America), he has published books and papers in various areas including electronic circuit design, nucleonics, biomedical electronics and gas sensors. He is a former Associate Editor for the *IEEE Sensors Journal*. He is also a qualified pilot.

Dr. Watson has served as Visiting Professor at the University of Calgary, Canada, and the University of California at both Davis and Santa Barbara; was External Examiner to the London University Postgraduate Department of Medical Electronics and Physics at St. Bartholomew's Hospital; and has held various consultancies with firms in the United States, Canada and Japan. Since retirement from Swansea University in the United Kingdom, he has continued as President of the UK-based Gas Analysis and Sensing Group.

Acknowledgments

The editors wish to thank the distinguished authors of this book, all of whom spent valuable time writing their chapters despite the already huge workloads dictated by their normal activities. The combination of their dedicated efforts has helped create a book that endeavors to cover as much as possible of such a rapidly developing and knowledge-based branch of technology as aerospace navigation systems and many of its current problems. We are extremely grateful to each member of this highly qualified international team of specialists, and hope that readers will also appreciate the sharing of their invaluable in-depth knowledge.

Especial gratitude is due to members of the IFAC Aerospace Technical Committee, particularly its present chairman, Prof. Shinichi Nakasuka, its former chairman Professor Houria Siguerdidjane, and Professor Klaus Schilling who is a member of the Steering Committee along with A.V. Nebylov.

The numerous colleagues of A.V. Nebylov, professors and researchers at the State University of Aerospace Instrumentation in St. Petersburg, also merit profound gratitude. They, along with several generations of students, have provided fruitful dialogues that have helped realize this vision of the problems inherent in the development and perfection of aerospace navigation systems.

We are also indebted to the Wiley editorial and production staff for their valued suggestions and constructive advice during the preparation of the manuscript.

Finally, we would like to thank our respective families, because work on the book has often been performed at the expense of time otherwise available for domestic companionship. Our wives, Elena and Margaret, respectively, have endured these difficulties with considerable forbearance.

Any criticism regarding the contents and material of the book and the quality of its presentation will be accepted with gratitude.

Alexander V. Nebylov
Joseph Watson

List of Contributors

Bijay Agarwal
Sattva E-Tech India Pvt Ltd.
Bangalore, India

Georgy V. Antsev
Concern Morinformsystem-Agat JSC
Moscow, Russia and
Radar-mms Research Enterprise JSC
Saint Petersburg, Russia

Anatoly V. Balov
Institute of Radionavigation and Time
Saint Petersburg, Russia

Michael S. Braasch
School of Electrical Engineering and Computer Science
Avionics Engineering Center
Ohio University
Athens, OH, USA

Sergey P. Faleev
State University of Aerospace Instrumentation
Saint Petersburg, Russia

Walter Geri
Magneti Marelli S.p.A., Bologna, Italy

Evgeny A. Konovalov
Late of the Russian Tsiolkovsky Academy of Cosmonautics
Moscow, Russia

Alexander V. Nebylov
State University of Aerospace Instrumentation
Saint Petersburg, Russia

Ron T. Ogan
Captain, U.S. Civil Air Patrol and Senior Member, IEEE
USA

Vladimir Y. Raspopov
Tula State University
Tula, Russia

Valentine A. Sarychev
Radar-mms Research Enterprise JSC
Saint Petersburg, Russia

Sukrit Sharan
Sattva E-Tech India Pvt Ltd.
Bangalore, India

Boris V. Shebshaevich
Institute of Radionavigation and Time
Saint Petersburg, Russia

J. Paul Sims
East Tennessee State University
Johnson City, TN, USA

Oleg A. Stepanov
Concern CSRI Elektropribor, JSC
ITMO University
Saint Petersburg, Russia

Joseph Watson
Swansea University (retd.)
Swansea, UK

Matteo Zanzi
Department of Electrical, Electronic and Information Engineering
“Guglielmo Marconi” (DEI)
University of Bologna, Bologna, Italy

Sergey P. Zarubin
Institute of Radionavigation and Time
Saint Petersburg, Russia

Preface

The generic term "aerospace vehicles" refers to both air and space vehicles, which is logical because they both imply the possibility of three-dimensional controlled motion, high maximum attainable speeds, largely similar methods and parameters of motion, and the need for accurate location measurement. This last aspect was the key factor in determining the title and content of this book.

The main difference between aerospace navigation sensors and systems is actually in the level of complexity. Usually, a system has several sensors and other integral elements (like an Inertial Navigation System or INS), or a set of airborne and ground components (like a radio navigation system); or a set of airborne and space-based elements (like a Satellite Navigation System or SNS), or is constructed using radar or photometry principles (like correlated-extremal systems or map-matching systems). However, the *raison d'être* for navigation sensors and navigation systems is the same—to give valuable and reliable information about changes in the navigation parameters of any aerospace vehicle. In fact, in an integrated navigation complex, all sensors and systems are elements of equal importance, each contributing to the navigational efficiency determined not by the complexity of the design, but by the dynamic properties and spectral characteristics of the measurement error.

It is precisely such properties of navigation systems that make them vastly important to investigate for ensuring high precision in navigation complexes—hence it is this wide-ranging material that is the main subject of the book. When selecting optimum sets of onboard navigational information sources, it is important to know their error properties, their reliabilities, their masses and indicator dimensions, and of course their cost effectiveness. The book also contains material on future prospects for the development of different types of navigation system and opportunities for improving their performances.

Seven different systems are considered, only one of which provides complete autonomous navigation under all conditions, though unfortunately for short periods only. This is the INS, which is based on a set of gyroscopes and accelerometers, various types of which are amongst the most well developed of all devices and are generically termed *inertial sensors*. These provide very wide choices for the INS designer from some extremely accurate versions such as fiber-optic and electrostatic gyros, to some very small and cheap sensors based on MEMS. Principles of INS design, algorithms of INS functioning, and estimations of achievable accuracy are described in Chapter 1, and special attention is paid to the strapdown INS: the most widely used of all aerospace navigation complexes.

Chapter 2 describes SNSs, which in recent years, have become the most common means of determining the positions and velocities of aerospace objects. Global SNS was literally a revolution in navigation and fundamentally changed the available capabilities. It became possible to reduce navigation errors in favorable cases down to several meters, and even (in phase mode) to decimeters and centimeters. However, because of the risk of integrity loss in the satellite measurements and the low interference immunity of satellite navigation, it is not possible to consider the use of SNS as a cardinal approach to satisfying the rapidly increasing requirements for accuracy and reliability in navigation measurements. For personal navigation in large cities, and especially for indoor navigation, the SNS may be complemented by local navigation systems based on electronic maps of Wi-Fi network signal availability. However, for most aerospace vehicles the needed addition to SNS is the use of time-proven classic radio navigation systems.

Chapter 3 describes long-range navigation systems that are extremely reliable but not very accurate in comparison with SNS. Networks for long-range radio navigation cover almost all conceivable aviation routes, making it possible to solve the problem of aircraft, including helicopters, determining their *en route* positions without an SNS receiver, or after losing the working capacity of an SNS.

Chapter 4 is devoted to short-range navigation systems for the very accurate and reliable positioning of aircraft in specific areas with high requirements for precision motion control, usually near airports. Such methods can also be used in aircraft or spacecraft rendezvous applications.

Chapter 5 describes the landing navigation systems that allow aircraft to accurately maintain descending and landing paths under the control of all the necessary movement parameters. Course, glide slope, and marker beacons within the VOR/DME system allow the generation of radio fields for the trajectory control of landing aircraft. The use of these well-established landing systems provides a high level of safety, and they are in the mandatory list of equipment for all higher category aerodromes.

All the radio navigation systems considered in Chapters 2–5 require the deployment of a set of numerous ground radio beacons for creating the artificial radio-fields that permit perfect aircraft navigation. However, in nature there also exist various natural fields exhibiting different physical parameters of the solid underlying surface of the Earth and of other planets, and which can also be used for accurate navigation. The height of the surface relief of the earth under a flying aircraft and its terrain shape are certainly informative parameters for navigation, and it is currently possible to measure such parameters with the help of onboard instruments and to compare their values with pre-prepared maps. There are also some other physical parameters, the actual values of which can be compared with the map values, whence the resulting information will give coordinates for an aircraft's location. These approaches are usually implemented by the principle of correlation-extreme image analysis. Navigation systems based on this principle are described in Chapter 6.

Chapter 7 is devoted to the homing systems that solve problems connected with the docking of two aerospace vehicles where, as for missile guidance, information about the relative position of one vehicle with respect to the other is needed. This information can be obtained on the basis of the principles of active or passive location in different electromagnetic radiation frequency ranges. Guidance systems are rapidly improving performance and becoming "smarter," these trends also being described in Chapter 7.

Chapter 8 describes different approaches to the design of the filtering algorithms used in integrated navigation systems with two or more sensors having different physical properties and principles of operation. The output signals of such sensors invariably need to be subjected to filtering in order to more effectively suppress the measurement error of each sensor. In the case of two different sensors, their outputs are usually passed through a low-pass and high-pass filter, respectively. However, the specific parameters of these filters must be chosen in accordance with the theory of optimal linear filtering; and recently, even nonlinear filtering has been quite frequently used. The synthesis of integrated navigation systems is one of the most popular testing procedures for developing and for checking the reliability of methods for optimal and suboptimal filtering, and it is this that dictated the advisability of devoting a complete chapter to the subject. Hence, the main variants of the filtering problem statement and the algorithms used for their solutions are included in this chapter.

Chapter 9 describes the modern navigational displays that are able to provide effective exchange of information between the crew and the automatic navigation systems of the aircraft. Such displays actually show the result of the entire piloting and navigation system operations. Both hardware and structural means of implementing these displays are shown for a wide class of aircraft including commercial, military, and general aviation categories to illustrate cockpit avionic systems of varying complexities.

Finally, Chapter 10 deals with the navigational requirements of unmanned aerospace vehicles (UAVs)—rapidly becoming generically known as "drones." It is intended to provide a basis for the understanding of new developments of this burgeoning field, which encompasses both civil and military applications.

The systems described throughout the book include those representing the complex and advanced types of technical innovation that made possible the remarkably high levels of development in navigation and motion control systems that occurred near the turn of the century. They are widely used in both civil and military aircraft as well as partially in space technology. In civil aviation, standards for the use of these instruments are determined by the ICAO, and common approaches are used in practically all countries of the world. In military aviation, such complete uniformity does not exist, but many of the design principles used by different developers are similar to each other because of parallel development resulting from the need to find the best technical solutions according to the basic physical principles utilized in the equipment operation. For example, the American GPS, the Russian GLONASS, and the European GALILEO are rather similar in their principles of construction.

Actually, the development of major hardware for aerospace navigation takes place largely in the United States, the European Union, and Russia, and each of these is represented by the present authors. The idea of the book was born during discussions amongst experts at meetings of the IFAC Aerospace Technical Committee, of which A.V. Nebylov is a member. Also, for many years he has been at the State University of Aerospace Instrumentation (SUAI) in St. Petersburg, Russia, which has made it convenient for him to choose several of the authors from the many scientific and manufacturing centers in that city. It was here where the fully automatic and very successful landing systems of the *Buran* (Snowstorm) aerospace plane (Russia's equivalent of America's Space Shuttle) were designed. The Western authors were located by J. Watson, who was also responsible for the

English language formatting of the entire volume. This second program of cooperation between the editors arose naturally from that resulting in a previous and related volume, *Aerospace Sensors* (Momentum Press, 2013).

The primary purpose of the book is to present the fundamentals of design, construction, and application of numerous aerospace navigation and guidance systems to engineers, designers, and researchers in the area of control systems for various aerospace vehicles including aircraft, UAVs, space planes, and missiles. However, it may also be used as a study guide for both undergraduate and graduate students and for postgraduates in aerospace engineering, avionics, aeronautics, astronautics, and various related areas. Finally, the editors hope that it might also be found useful by many other people wishing to satisfy their general interest in modern aerospace technology.

1

Inertial Navigation Systems

Michael S. Braasch
School of Electrical Engineering and Computer Science, Avionics Engineering Center, Ohio University, Athens, OH, USA

1.1 Introduction

Inertial Navigation Systems (INSs) are modern, technologically sophisticated implementations of the age-old concept of dead reckoning. The basic philosophy is to begin with a knowledge of initial position, keep track of speed and direction, and thus be able to determine position continually as time progresses. As the name implies, the fundamental principle involved is the property of inertia. Specifically, a body at rest tends to stay at rest and a body in motion tends to stay in motion unless acted upon by an external force.

From Newton's second law of motion, the well-known relation can be derived:

$$\vec{F} = m\vec{a} \tag{1.1}$$

where "$\vec{F}$" is a force vector, "m" is mass, and "$\vec{a}$" is the acceleration vector. Conceptually, it is then possible to measure force and subsequently determine acceleration. This may then be integrated to determine velocity, which in turn may be integrated to determine position.

Each accelerometer described in chapter 5 of the companion volume, *Aerospace Sensors* (Konovalov, 2013), can determine a measure of linear acceleration in a single dimension, from which it follows that multiple accelerometers are needed to determine motion in the general three-dimensional case. However, in addition, it is necessary to determine the direction in which the accelerometers are pointing, which is not a trivial exercise considering that an aircraft can rotate around three axes. If the accelerometers are hard-mounted to the vehicle (as is typically the case), then theoretically they can be oriented in any direction. Double integration of their outputs is useless if this time-varying orientation is not properly taken into account.

The determination of orientation (also known as attitude determination) is accomplished through processing of data from the gyroscopes described in chapter 6 on *Aerospace Sensors* (Branets *et al.*, 2013). These devices measure either angular rate and/or angular displacement.

Aerospace Navigation Systems, First Edition. Edited by Alexander V. Nebylov and Joseph Watson.

So-called navigation-grade gyros can measure angular rate with accuracies on the order of 0.01°/h. Such sensors are needed to determine attitude to permit velocity and position determination in a given reference frame.

There are two main types of INSs: gimbaled and strapdown (Lawrence, 1998). In a gimbaled system, the accelerometers are mounted on a platform that is rotationally isolated from the vehicle. This platform is maintained in a local-level orientation so that there are two accelerometers in the horizontal plane for providing the data needed to compute horizontal velocity and position. In a strapdown system, the accelerometers are hard-mounted to the vehicle itself. Gimbaled systems are mechanically complex but do not require intensive computational capability. Strapdown systems are mechanically simple but require more intensive computations to deal with the time-varying orientation of the vehicle. Throughout the remainder of this chapter, strapdown operation will be assumed because modern processors are in no way challenged by the computational requirements. Furthermore, the simplified mechanical design (along with modern optical gyros) yields systems with Mean Time Between Failures (MTBFs) measured in tens of thousands of operational hours (versus the hundreds of hours that were typical of gimbaled systems in the late 1970s).

1.2 The Accelerometer Sensing Equation

Equation 1.1 stated the well-known relationship between force and acceleration. Solving for acceleration yields the following equation:

$$\frac{\vec{F}}{m} = \vec{a} \tag{1.2}$$

The quantity on the left is referred to as "specific force" and is what an accelerometer inherently measures. However, in the presence of a gravitational field, the specific force measured by an accelerometer is not equal to the classic Newtonian acceleration. As an example, the pendulous accelerometers described by Konovalov in chapter 5 of *Aerospace Sensors* have pendulums that displace under acceleration because of inertia. However, even if a sensor is stationary, the pendulum will still displace due to the effects of gravity. Specifically, the pendulum will displace downward just as it would have if the device were actually accelerating upward. Accelerometers thus measure the combination of Newtonian acceleration and the reaction force to gravity:

$$\vec{f} = \vec{a} - \vec{g} \tag{1.3}$$

where $\vec{f}$ is the measured specific force vector, $\vec{a}$ is the Newtonian acceleration vector, and $\vec{g}$ is the earth's gravity vector. This is the so-called accelerometer sensing equation. The desired Newtonian acceleration vector is thus given by the following equation:

$$\vec{a} = \vec{f} + \vec{g} \tag{1.4}$$

Although the equation is quite simple, it reveals a fundamental concept in inertial navigation. In order to determine acceleration from specific force, the inertial system needs to determine the value of the gravity vector at its current position because the value of this gravity vector varies significantly with position and especially with altitude. A variety of gravity models have been developed over the past 60 years, and the ones typically utilized in inertial navigation have accuracies on the order of 5–10 μg (i.e., five to ten one-millionths the average magnitude of gravity at the earth's surface) (Hsu, 1998).

1.3 Reference Frames

A variety of coordinate (or reference) frames are utilized in INSs (Britting, 1971). Accelerometers and gyros form their measurements with respect to inertial space (i.e., the inertial frame), but they output their data with respect to frames that are fixed to the vehicle. Furthermore, velocity is typically expressed in east/north/up components (i.e., a local-level reference frame), and position is frequently expressed in terms of latitude and longitude (i.e., a reference frame fixed to the Earth). It is therefore important to understand these various reference frames and then to understand how to take quantities expressed in one frame and convert them to another.

1.3.1 True Inertial Frame

The true inertial frame is given by any reference frame that does not accelerate with respect to the stars in the galaxy in which Earth resides—the Milky Way. Classical physics has established these "fixed stars" as an acceptable inertial reference frame (i.e., a frame in which Newton's laws are valid).

1.3.2 Earth-Centered Inertial Frame or i-Frame

The Earth-Centered Inertial Frame (ECI), or i-frame, is a frame that is centered in the Earth but does not rotate with it—its orientation with respect to the stars remains fixed. This frame is not truly inertial since the Earth revolves around the Sun, and hence the i-frame undergoes nonzero acceleration with respect to the stars. However, for navigation tasks on or near the surface of the Earth, this acceleration can be considered negligible.

1.3.3 Earth-Centered Earth-Fixed Frame or e-Frame

The Earth-Centered Earth-Fixed (ECEF) frame, or e-frame, is also a frame that is centered in the Earth, but is also fixed to it. Hence, it rotates along with the Earth. Two of the axes are in the equatorial plane, and the third axis is aligned with the nominal pole of rotation of the Earth. Although the choice for the equatorial plane axes is arbitrary, one of the most common specifies an x-axis that intersects the prime meridian (through Greenwich, UK).

1.3.4 Navigation Frame

The navigation frame, or n-frame, is centered in the vehicle, but it does not rotate with the vehicle—it remains at a local level. The choice of the horizontal plane axes is arbitrary, but one of the most common specifies an x-axis that points north, a y-axis that points east, and a z-axis that points "down" (i.e., approximately along the gravity vector). This particular

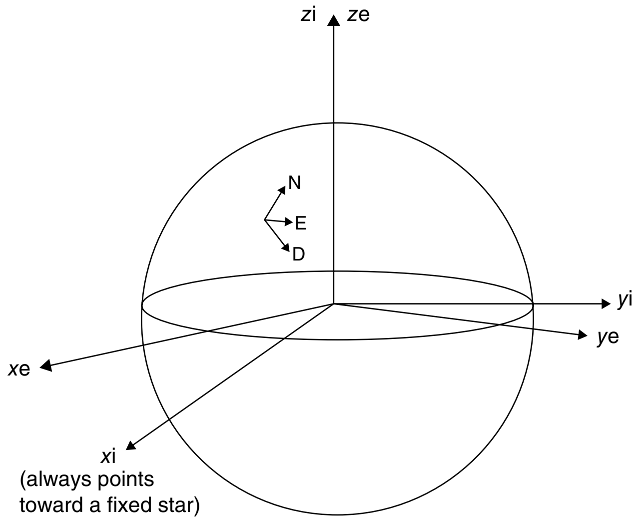

Figure 1.1 Depiction of i-frame, e-frame, and n-frame

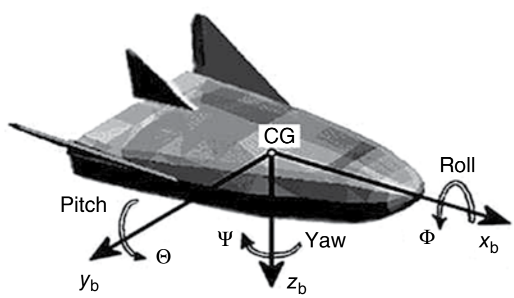

Figure 1.2 Depiction of b-frame (reprinted, with permission from Depiction of b-frame reprinted by permission of Nebylov, A. V., chapter 1, p. 7, "Introduction," *Aerospace Sensors*, Momentum Press, LLC, New York, 2013)

convention is sometimes referred to as the "north–east–down" or "NED" frame. However, in some cases it is desirable not to force the local-level frame to have an axis pointing north. When the local-level frame is permitted to rotate (around the vertical) away from north, the resulting frame is sometimes referred to as a "wander frame." The angle of rotation around the vertical is known as the "wander angle" and is typically denoted by α. The i-, e-, and n-frames are depicted in Figure 1.1.

1.3.5 Body Frame

The body frame, or b-frame, is centered in the vehicle and is fixed to it (Figure 1.2) (Nebylov, 2013). It is typically specified to coincide with the principal axes of the vehicle. For an aircraft, the convention is chosen such that the x-axis aligns with the longitudinal axis of the vehicle (positive out of the nose), the *y*-axis points out of the right wing, and the *z*-axis points out of the bottom of the vehicle (i.e., “down” if the vehicle is level). This convention is therefore such that positive rotations about these axes correspond to positive Euler angles (roll, pitch, and yaw).

1.3.6 Sensor Frames (a-Frame, g-Frame)

The sensor frames are specified by orthogonal sensor triads. An orthogonal set of three accelerometers forms the a-frame, and an orthogonal set of gyroscopes forms the g-frame. The a- and g-frames are not coincident since it is physically impossible to mount both the accelerometers and the gyros in exactly the same space. Furthermore, the sensor triads are typically not mounted in perfect alignment with the b-frame. In fact, for installation convenience, it is not uncommon to have large angular offsets between the sensor frames and the b-frame. For the remainder of this chapter, however, it will be assumed that the offsets have been determined during installation and that the sensor outputs have been converted to their b-frame equivalents.

1.4 Direction Cosine Matrices and Quaternions

A variety of coordinate frame conversions are utilized in inertial navigation. For example, accelerometer outputs expressed in the b-frame need to be converted to the n-frame before velocity and position can be computed. It is assumed the reader is already familiar with the concept of rotation matrices, so only the key relationships for inertial navigation will be summarized here. For a more detailed discussion of the fundamental concepts, the reader is directed to Kuipers (2002).

A vector expressed in the b-frame may be converted to the n-frame as follows:

$$\vec{f}^{\mathrm{n}} = C_{\mathrm{b}}^{\mathrm{n}} \vec{f}^{\mathrm{b}} \tag{1.5}$$

where the so-called body-to-navigation direction cosine matrix (DCM) is given by the following equation:

$$C_{\mathrm{b}}^{\mathrm{n}} = \begin{bmatrix} \cos\theta\cos\psi & -\cos\phi\sin\psi + \sin\phi\sin\theta\cos\psi & \sin\phi\sin\psi + \cos\phi\sin\theta\cos\psi \\ \cos\theta\sin\psi & \cos\phi\cos\psi + \sin\phi\sin\theta\sin\psi & -\sin\phi\cos\psi + \cos\phi\sin\theta\sin\psi \\ -\sin\theta & \sin\phi\cos\theta & \cos\phi\cos\theta \end{bmatrix} \tag{1.6}$$

where:

ϕ = roll angle

θ = pitch angle

ψ = yaw angle

This DCM defines the orientation (attitude) of the vehicle by specifying the rotational difference between the local-level n-frame and the fixed-to-the-vehicle b-frame; and the initialization and updating of this matrix will be discussed later in this chapter. Although there are nine elements in the matrix, only six of them need to be updated (the other three can be derived from the orthonormality property of the matrix). As discussed in Kuipers (2002), an equivalent attitude representation is given by the quaternion. Quaternions have only four elements and thus are more efficient than DCMs that need at least six elements to be specified uniquely. Again, both representations are equivalent and the remainder of this chapter will consider only DCMs for attitude representation.

The rotational differences between the Earth frame and the n-frame are given by the latitude, longitude, and (optionally) the wander angle and are expressed in the Earth-to-nav DCM:

$$C_{\mathrm{e}}^{\mathrm{n}} = \begin{bmatrix} -\cos\alpha\sin\mathrm{Lat}\cos\mathrm{Lon} - \sin\alpha\sin\mathrm{Lon} & -\cos\alpha\sin\mathrm{Lat}\sin\mathrm{Lon} + \sin\alpha\cos\mathrm{Lon} & \cos\alpha\cos\mathrm{Lat} \\ \sin\alpha\sin\mathrm{Lat}\cos\mathrm{Lon} - \cos\alpha\sin\mathrm{Lon} & \sin\alpha\sin\mathrm{Lat}\sin\mathrm{Lon} + \cos\alpha\cos\mathrm{Lon} & -\sin\alpha\cos\mathrm{Lat} \\ -\cos\mathrm{Lat}\cos\mathrm{Lon} & -\cos\mathrm{Lat}\sin\mathrm{Lon} & -\sin\mathrm{Lat} \end{bmatrix} \tag{1.7}$$

where:

α = wander angle

Lat = latitude

Lon = longitude

Since DCMs are orthonormal matrices, their inverse is equal to their transpose:

$$C_{\mathrm{n}}^{\mathrm{b}} = \left(C_{\mathrm{b}}^{\mathrm{n}}\right)^{-1} = \left(C_{\mathrm{b}}^{\mathrm{n}}\right)^{T}$$
$$C_{\mathrm{n}}^{\mathrm{e}} = \left(C_{\mathrm{e}}^{\mathrm{n}}\right)^{-1} = \left(C_{\mathrm{e}}^{\mathrm{n}}\right)^{T}$$

1.5 Attitude Update

The accelerometer outputs expressed in the b-frame need to be resolved into a frame of interest for subsequent updating of the vehicle velocity and position states. For aircraft applications, the frame of interest is usually the n-frame. As described in the previous section, the body-to-nav DCM can be used to perform this conversion. However, this DCM needs to be updated continuously to account for rotations of both the b-frame and the n-frame.

The two rotations are driven by two corresponding angular rates:

$\vec{\omega}_{\mathrm{ib}}^{\mathrm{b}}$ = angular rate of the b-frame, relative to the i-frame, expressed in b-coordinates

$\vec{\omega}_{\mathrm{in}}^{\mathrm{n}}$ = angular rate of the n-frame, relative to the i-frame, expressed in n-coordinates

The differential equation governing the rate of change of the body-to-nav DCM is given by the following equation (Titterton and Weston, 2005):

$$\dot{C}_{\mathrm{b}}^{\mathrm{n}} = C_{\mathrm{b}}^{\mathrm{n}}\left[\vec{\omega}_{\mathrm{ib}}^{\mathrm{b}}\times\right] - \left[\vec{\omega}_{\mathrm{in}}^{\mathrm{n}}\times\right]C_{\mathrm{b}}^{\mathrm{n}} \tag{1.8}$$

where:

$$\left[\vec{\omega}_{\mathrm{ib}}^{\mathrm{b}}\times\right] = \text{skew symmetric matrix form of the body-rate vector } \vec{\omega}_{\mathrm{ib}}^{\mathrm{b}}$$

$$= \begin{bmatrix} 0 & -\omega_{\mathrm{ib}}^{\mathrm{b}}(z) & \omega_{\mathrm{ib}}^{\mathrm{b}}(y) \\ \omega_{\mathrm{ib}}^{\mathrm{b}}(z) & 0 & -\omega_{\mathrm{ib}}^{\mathrm{b}}(x) \\ -\omega_{\mathrm{ib}}^{\mathrm{b}}(y) & \omega_{\mathrm{ib}}^{\mathrm{b}}(x) & 0 \end{bmatrix}$$

$$\left[\vec{\omega}_{\mathrm{in}}^{\mathrm{n}}\times\right] = \text{skew symmetric matrix form of the n-frame-rate vector } \vec{\omega}_{\mathrm{in}}^{\mathrm{n}}$$

$$= \begin{bmatrix} 0 & -\omega_{\mathrm{in}}^{\mathrm{n}}(z) & \omega_{\mathrm{in}}^{\mathrm{n}}(y) \\ \omega_{\mathrm{in}}^{\mathrm{n}}(z) & 0 & -\omega_{\mathrm{in}}^{\mathrm{n}}(x) \\ -\omega_{\mathrm{in}}^{\mathrm{n}}(y) & \omega_{\mathrm{in}}^{\mathrm{n}}(x) & 0 \end{bmatrix}$$

Since the angular rate of the body can be very high (e.g., hundreds of degrees per second for aerobatic aircraft) and the n-frame rate is very low (as will be discussed later), the DCM update is performed in two parts: one for the b-frame update and the other for the n-frame update.

1.5.1 Body Frame Update

The rotation of the b-frame relative to the inertial frame is measured by the gyros. The discrete-time update of the body-to-nav DCM accounting for body rotation is given by the following equation (Titterton and Weston, 2005):

$$C_{\mathrm{b}[k+1]}^{\mathrm{n}} = C_{\mathrm{b}[k]}^{\mathrm{n}} e^{[\vec{\sigma}\times]} \tag{1.9}$$

where:

$$k = \text{time index}$$

$$[\vec{\sigma}\times] = \text{skew symmetric matrix form of the rotation vector } \vec{\sigma}$$

$$= \begin{bmatrix} 0 & -\sigma_z & \sigma_y \\ \sigma_z & 0 & -\sigma_x \\ -\sigma_y & \sigma_x & 0 \end{bmatrix}$$

The components of the rotation vector are computed from the gyro outputs. If the body angular rate vector had a fixed orientation, the rotation vector could be computed very simply as follows:

$$\vec{\sigma} \approx \int_{t_k}^{t_{k+1}} \vec{\omega}_{\mathrm{ib}}^{\mathrm{b}} dt \tag{1.10}$$

However, in practice the body angular-rate vector changes orientation, at least in part, because of vibration. On a larger scale, this change can also occur when an aircraft is performing so-called S-turns (Kayton and Fried, 1997). The change of angular rate vector orientation is referred to as "coning." The term refers to the geometric figure of a cone being swept out by the axis of rotation. When this occurs during the interval in which the angular rate is being integrated, an erroneous angular displacement will be computed. As a result, a coning compensation algorithm is applied in the computation of the rotation vector (Ignagni, 1996).

Before continuing, it should be noted that the matrix exponential in Equation 1.9 is typically approximated using the first few terms of a Taylor series expansion.

1.5.2 Navigation Frame Update

The rotation of the n-frame, relative to the inertial frame, is a function of two rotations: Earth rate and transport rate:

$$\vec{\omega}_{\mathrm{in}}^{\mathrm{n}} = \vec{\omega}_{\mathrm{ie}}^{\mathrm{n}} + \vec{\omega}_{\mathrm{en}}^{\mathrm{n}} \tag{1.11}$$

This rotation rate of the n-frame is also known as "spatial rate." The two components will now be described.

1.5.2.1 Earth Rate

Even if the vehicle is stationary relative to the Earth, the n-frame must rotate relative to the i-frame, at the earth's rotation rate, in order for it to stay locally level.

$$\begin{aligned}
\vec{\omega}_{\mathrm{ie}}^{\mathrm{n}} &= C_{\mathrm{e}}^{\mathrm{n}} \vec{\omega}_{\mathrm{ie}}^{\mathrm{e}} \\
\vec{\omega}_{\mathrm{ie}}^{\mathrm{e}} &= \begin{bmatrix} 0 & 0 & \omega_{\mathrm{ie}} \end{bmatrix}^T \\
\omega_{\mathrm{ie}} &\approx 7.292115e-5 \text{ rad/s}
\end{aligned}$$

1.5.2.2 Transport Rate

Furthermore, if the vehicle is moving relative to the Earth, then to stay at a local level the n-frame must also rotate to account for the motion of the vehicle over the surface of the curved Earth. This is obviously a function of the horizontal velocity components. For north-pointing mechanizations, the transport-rate vector is given by (Kayton and Fried, 1997; Titterton and Weston, 2005):

$$\vec{\omega}_{\mathrm{en}}^{\mathrm{n}} = \begin{bmatrix} \dfrac{V_{\mathrm{E}}}{R_{\mathrm{P}} + h} & -\dfrac{V_{\mathrm{N}}}{R_{\mathrm{M}} + h} & -\dfrac{V_{\mathrm{E}} \tan \mathrm{Lat}}{R_{\mathrm{P}} + h} \end{bmatrix}^T \tag{1.12}$$

where:

V_{E} = east component of velocity
V_{N} = north component of velocity
h = altitudue
R_{M} = radii of curvature of the earth in the north-south direction (also known as the meridian radius of curvature)

$$= \frac{a\left(1-e^2\right)}{\left(1-e^2 \sin^2 \mathrm{Lat}\right)^{3/2}}$$

$R_p =$ radii of curvature of the earth in the east-west direction (also known as the prime radius of curvature)

$$= \frac{a}{\left(1 - e^2 \sin^2 \mathrm{Lat}\right)^{1/2}}$$

a = semi-major axis of the earth ellipsoid (i.e., Equatorial radius)
e = eccentricity of the earth ellipsoid

It should be noted that the vertical component of transport rate has a singularity at the earth's poles. Specifically, the term "tan(Lat)" approaches infinity as latitude approaches ±90°. This is not an issue for vehicles that stay in mid-latitude or equatorial regions. For polar or near-polar crossings, however, north-pointing mechanizations must be replaced with a wander-azimuth mechanization that does not force one of the n-frame axes to point in the north direction (Jekeli, 2000).

1.5.2.3 Navigation-Frame Update Algorithm

The magnitude of the spatial rate vector is very small. Even for commercial jets traveling at 500 knots, it can be shown that the magnitude of transport-rate is approximately half of Earth rate. As a result, a simple trapezoidal approximation of the discrete-time update is generally acceptable:

$$C_{\mathrm{b}}^{\mathrm{n}[k+1]} = \left\{ I - \frac{1}{2}\left(\left[\vec{\omega}_{\mathrm{in}}^{\mathrm{n}}(t_k)\times \right] + \left[\vec{\omega}_{\mathrm{in}}^{\mathrm{n}}(t_{k+1})\times \right] \right)\Delta t \right\} C_{\mathrm{b}}^{\mathrm{n}[k]} \tag{1.13}$$

where:

$\left[\vec{\omega}_{\mathrm{in}}^{\mathrm{n}}(t_k)\times \right] =$ skew symmetric matrix form of $\vec{\omega}_{\mathrm{in}}^{\mathrm{n}}$ at time t_k

$\Delta t = t_{k+1} - t_k$

1.5.3 Euler Angle Extraction

Once the body-to-nav DCM has been updated for both b-frame and n-frame rotations, it may be used to convert accelerometer outputs as shown in Equation 1.5. It should also be noted that the updated DCM inherently contains the updated representation of the attitude of the vehicle or inertial system. From Equation 1.6, it follows that the Euler angles can be extracted from the updated DCM as follows:

$$\begin{aligned} \phi &= \arctan 2\left(C_{\mathrm{b}}^{\mathrm{n}}(3,2), C_{\mathrm{b}}^{\mathrm{n}}(3,3) \right) \\ \theta &= \arcsin\left(-C_{\mathrm{b}}^{\mathrm{n}}(3,1) \right) \\ \psi &= \arctan 2\left(C_{\mathrm{b}}^{\mathrm{n}}(2,1), C_{\mathrm{b}}^{\mathrm{n}}(1,1) \right) \end{aligned} \tag{1.14}$$

Note: the four-quadrant arc-tangent functions are needed to preserve the full range of roll and yaw angles.

1.6 Navigation Mechanization

The differential equation governing the rate of change of the velocity vector is given by

$$\dot{v}_{\mathrm{e}}^{\mathrm{n}} = C_{\mathrm{b}}^{\mathrm{n}} \vec{f}^{\mathrm{b}} - \left[2\vec{\omega}_{\mathrm{ie}}^{\mathrm{n}} + \vec{\omega}_{\mathrm{en}}^{\mathrm{n}}\right] \times \vec{v}_{\mathrm{e}}^{\mathrm{n}} + \vec{g}_{\mathrm{eff}}^{\mathrm{n}} \tag{1.15}$$

where the cross-product term accounts for the effects of Coriolis on the rotating Earth and n-frames and where

$$\vec{g}_{\mathrm{eff}}^{\mathrm{n}} = \vec{g}^{\mathrm{n}} - \vec{\omega}_{\mathrm{ie}}^{\mathrm{n}} \times \vec{\omega}_{\mathrm{ie}}^{\mathrm{n}} \times \vec{R}$$

is known as “effective gravity,” “apparent gravity,” “local gravity,” or “plumb-bob gravity.” It is the combination of the earth’s mass attraction (first term) and centripetal acceleration due to Earth rotation (vector triple-product term $\vec{R}$ is the position vector with origin at the center of the Earth). To the first order, effective gravity is aligned with the local vertical (note that since the Earth is ellipsoidal, extension of the local vertical down to the equatorial plane does not intersect the mass center of the Earth, unless one is located at the poles or on the equator).

Conceptually, the Coriolis term may be understood as follows: Consider a vehicle that starts at the North Pole and travels due south along a meridian (path of constant longitude). Relative to the Earth, the horizontal path is “straight” (i.e., no east–west motion). However, relative to the i-frame, the path is clearly curved due to the rotation of the Earth. The inertial sensors detect the actual curved path in space, but the Coriolis term allows the overall equation to compute a velocity relative to the Earth, not relative to the inertial frame.

The discrete-time update associated with 1.14 is very straightforward:

$$v_{\mathrm{e}}^{\mathrm{n}}[k+1] = v_{\mathrm{e}}^{\mathrm{n}}[k] + C_{\mathrm{b}}^{\mathrm{n}} \overrightarrow{\Delta V}_k^{\mathrm{b}} + \left\{-\left[2\vec{\omega}_{\mathrm{ie}}^{\mathrm{n}} + \vec{\omega}_{\mathrm{en}}^{\mathrm{n}}\right] \times \vec{v}_{\mathrm{e}}^{\mathrm{n}}[k] + \vec{g}_{\mathrm{eff}}^{\mathrm{n}}[k]\right\} \Delta t \tag{1.16}$$

where:

$$\overrightarrow{\Delta V}_k^{\mathrm{b}} \approx \int_{t_k}^{t_{k+1}} \vec{f}^{\mathrm{b}} dt$$

The integration of the specific force vector can be performed numerically if necessary, but some accelerometers perform this integration as part of their normal operation. For high-accuracy applications, two corrections need to be included in this specific force integration: sculling and size effect. Sculling error arises when an accelerometer is swinging back and forth at the end of a pendulum. This combination of rotation and acceleration results in a nonzero net sensed acceleration even though the average displacement of the accelerometer is zero. In practice, this motion occurs due to vibration. Sculling error can be corrected with a compensation algorithm that utilizes both the accelerometers' outputs and the coning-compensated gyro outputs (Mark and Tazartes, 1996; Savage, 1998). Alternatively, sculling error may be avoided by transforming the accelerometer outputs to the n-frame at a rate significantly higher than the highest anticipated vibration frequencies (Kayton and Fried, 1997).

Size-effect errors result from the nonzero lever arms between the three orthogonal accelerometers. Since the three sensors are not physically located in exactly the same point, they will sense different accelerations when the vehicle is rotating as well as accelerating. For high accuracy applications, a size-effect correction must be applied to the accelerometer outputs (Savage, 2009).

1.7 Position Update

The nav-to-Earth DCM is the transpose (also inverse) of the Earth-to-nav DCM. The differential equation governing the rate of change of the nav-to-Earth DCM is given by the following equation:

$$\dot{C}_{\mathrm{n}}^{\mathrm{e}} = C_{\mathrm{n}}^{\mathrm{e}} \left[\vec{\omega}_{\mathrm{en}}^{\mathrm{n}} \times \right] \tag{1.17}$$

The discrete-time update is then given by the following equation:

$$C_{\mathrm{n}}^{\mathrm{e}} \left[k+1 \right] = C_{\mathrm{n}}^{\mathrm{e}} \left[k \right] e^{\left[\vec{\zeta} \times \right]} \tag{1.18}$$

$$\begin{aligned} \left[\vec{\zeta} \times \right] &= \text{skew} - \text{symmetric matrix form of } \vec{\zeta} \\ &= \begin{bmatrix} 0 & -\zeta_z & \zeta_y \\ \zeta_z & 0 & -\zeta_x \\ -\zeta_y & \zeta_x & 0 \end{bmatrix} \\ \vec{\zeta} &= \int_{t_k}^{t_{k+1}} \vec{\omega}_{\mathrm{en}}^{\mathrm{n}} \, dt \end{aligned}$$

Again, the matrix exponential is typically approximated using the first few terms of the Taylor series expansion. The integration of the transport rate vector is typically performed either with rectangular or trapezoidal integration.

Once the DCM has been updated, the transpose is taken:

$$C_{\mathrm{e}}^{\mathrm{n}} = \left(C_{\mathrm{n}}^{\mathrm{e}} \right)^T$$

Finally, based on Equation 1.7, the position angles may be extracted as follows:

$$\begin{aligned} \text{Lon} &= \arctan 2\left(-C_{\mathrm{e}}^{\mathrm{n}}(3,2), -C_{\mathrm{e}}^{\mathrm{n}}(3,1)\right) \\ \text{Lat} &= \arcsin\left(-C_{\mathrm{e}}^{\mathrm{n}}(3,3)\right) \\ \alpha &= \arctan 2\left(-C_{\mathrm{e}}^{\mathrm{n}}(2,3), C_{\mathrm{e}}^{\mathrm{n}}(1,3)\right) \end{aligned} \tag{1.19}$$

Over short intervals of time, altitude may be determined by the following equation:

$$h_{k+1} = h_k + \int_{t_k}^{t_{k+1}} -v_{\mathrm{e}}^{\mathrm{n}}(z)\,dt \tag{1.20}$$

As will be discussed later, however, the vertical channel of an INS is inherently unstable and hence is unusable over long periods of time.

1.8 INS Initialization

The discrete-time updates for attitude, velocity, and position were given in Equations 1.9, 1.13, 1.16, 1.17, and 1.19. Each equation assumes that the quantity to be updated was known at the previous time step. Hence, these equations do not explain how attitude, velocity, and position are initialized.

Initial position is generally determined in one of two ways. For stationary vehicles, initial position can be determined by parking the vehicle at a known, surveyed location. At international airports, for example, travelers may see signs (visible to pilots from the cockpit) specifying the latitude, longitude, and altitude of a given gate. For vehicles that are in motion, initial position typically is provided through the use of a radio navigation aid such as GPS or GLONASS. For stationary vehicles, initial velocity may be specified as zero and, again, for vehicles in motion, external radio navigation aids may be utilized.

The most challenging aspect of initialization lies in the determination of the body-to-nav DCM. This amounts to the determination of the local level plane (from which roll and pitch are determined) and the determination of the direction of north (from which yaw or heading is determined).

Conceptually, the process of attitude determination is most easily understood in the context of a gimbaled INS. For a stationary vehicle, the only force sensed by the accelerometers is the force of gravity and, to first order, the gravity vector lies along the local vertical. The leveling process in a gimbaled system involves rotating the platform until the two accelerometers with sensitive axes in the platform plane are outputting zero (and thus are orthogonal to the gravity vector). In practice, all accelerometers output noise regardless of the value of the true sensed specific force, which is therefore averaged over a finite interval of time. For strapdown inertial systems, leveling is performed in two parts: coarse leveling and fine leveling.

Coarse leveling amounts to the estimation of pitch and roll by processing accelerometer outputs that have been averaged over a brief interval of time (i.e., a few seconds) (Kayton and Fried, 1997):

$$\begin{aligned}\phi &\approx a\tan\left(\frac{A_y^{\mathrm{b}}}{A_z^{\mathrm{b}}}\right)\\ \theta &\approx a\tan\left(\frac{A_x^{\mathrm{b}}}{\sqrt{\left(A_y^{\mathrm{b}}\right)^2+\left(A_z^{\mathrm{b}}\right)^2}}\right)\end{aligned} \tag{1.21}$$

where "A" is the averaged accelerometer output.

Given an initial estimate of level, the direction of north (or equivalently, platform heading or yaw angle) can be achieved by exploiting the fact that a stationary vehicle only experiences rotation due to the rotation of the Earth, that is, the gyros will only sense Earth rate. This is significant because Earth rate only has north and vertical components (i.e., there is no east component of Earth rate). The procedure works as follows. With the coarse estimation of roll and pitch, a coarse body-to-local-level DCM can be formed:

$$C_{\mathrm{b}}^{\mathrm{LL}}(\theta,\phi)\Big|_{\psi=0}=\begin{bmatrix}\cos\theta & \sin\phi\sin\theta & \cos\phi\sin\theta\\ 0 & \cos\phi & -\sin\phi\\ -\sin\theta & \sin\phi\cos\theta & \cos\phi\cos\theta\end{bmatrix}$$

With this coarse body-to-local-level DCM, the gyro outputs (which are only sensing Earth rate) can be transformed from the b-frame to the local-level frame:

$$\vec{\omega}_{\mathrm{ie}}^{\mathrm{LL}}=C_{\mathrm{b}}^{\mathrm{LL}}\vec{\omega}_{\mathrm{ie}}^{\mathrm{b}}$$

The level components of the sensed Earth rate are actually components of the north component of Earth rate (there being no east component of Earth rate). Thus, heading or yaw can be determined by (Kayton and Fried, 1997):

$$\psi \approx \arctan 2\left(\frac{-\omega_{\mathrm{ie}}^{\mathrm{LL}}(y)}{\omega_{\mathrm{ie}}^{\mathrm{LL}}(x)}\right) \tag{1.22}$$

Again, the gyro outputs are very noisy, so averaging is necessary before Equation 1.24 is computed.

The aforementioned procedure provides coarse initialization of roll, pitch, and yaw (or equivalently, the body-to-nav DCM). Fine leveling and yaw/azimuth determination typically involve the use of a Kalman filter and the exploitation of the knowledge that the velocity (of a stationary vehicle) is zero. The fine initialization Kalman filter is generally of the same type as that used to integrate external radio navigation aid information while the vehicle is in motion.

1.9 INS Error Characterization

INSs are subject to a wide variety of errors. These include mounting errors, initialization errors, sensor errors, gravity model errors, and computational errors, all of which are briefly described in the following text.

1.9.1 Mounting Errors

These include nonorthogonality of the sensor triads, unknown angular offsets between the sensor triads and reference points on the system case (that houses the sensors), and unknown angular offsets between the system case and the vehicle in which it is installed. The bulk of the nonorthogonality of the sensor triads and the angular offsets between the triads and the system case are determined during factory calibration, and the raw sensor outputs are compensated accordingly. Determination of the angular offsets between the inertial system case and the vehicle (i.e., the b-frame) is referred to as "boresighting" and is performed when the inertial system is initially mounted in the vehicle. Boresighting errors affect the accuracy of the Euler angles (roll, pitch, and yaw).

1.9.2 Initialization Errors

Initialization errors are the errors in the determination of initial position, velocity, and attitude. In the absence of external aiding, navigation-grade inertial systems (i.e., inertial systems capable of stand-alone positioning with drift rates on the order of 1 nautical mile per hour of operation) require accuracy of initial pitch and roll to be better than 0.1 mrad, initial azimuth better than 1 mrad, and initial velocity better than 0.5 m/s.

1.9.3 Sensor Errors

A variety of errors affect the performances of accelerometers and gyros and are discussed more fully in Konovalov and Branets (chapters 5 and 6 of *Aerospace Sensors* 2013). The primary sensor errors affecting INS performance are residual biases. These are the bias errors that remain after calibration/compensation and are different each time a given sensor is powered on. A secondary effect is scale factor error. The inherent noise in the sensors primarily drives the amount of filtering/averaging required during initialization.

1.9.4 Gravity Model Errors

A variety of closed-form gravity models exist (Hsu, 1998), which provide accuracies on the order of 5–10 μg. However, none is able to characterize the so-called deflection of the vertical because the actual direction of the gravity vector at the surface of the Earth is not perfectly orthogonal to the surface of the reference ellipsoid (i.e., the imaginary surface that defines zero altitude). The true gravity vector has nonzero horizontal components with magnitudes on the order of a few micro-gs. These values are position-dependent and vary greatly, for example, in mountainous regions. Though precise characterization of the gravity field can be accomplished using extensive look-up tables, for the vast majority of inertial navigation applications the closed-form models are sufficiently accurate.

1.9.5 Computational Errors

As discussed earlier in this chapter, inertial navigation algorithms require a variety of numerical methods including transcendental function approximation and numerical integration. When strapdown systems were being developed in the 1970s, computational power was limited, and the approximations needed to achieve real-time operation had a nontrivial impact on system performance. With the capabilities of modern processors, however, computational errors can be made negligible.

1.9.6 Simulation Examples

A detailed analysis of error sources may be found in Titterton and Weston (2005). Simulation results will be presented in this section to illustrate the impact of key error sources. The INS is simulated in a vehicle located at 45° North latitude, is level, and is pointed northward.

1.9.6.1 Accelerometer Bias Simulation

In this example, a 100 μg bias is simulated on the body x-axis accelerometer. Since the vehicle is level and is pointed northward, this accelerometer is sensitive in the north direction (Figures 1.3 and 1.4).

As would be expected with a bias on an accelerometer that is pointed north, the dominant errors are north position error and north velocity error along with pitch (since the vehicle is level and is also pointed north). The periodicity of the errors is known as the "Schuler period" and is approximately 84.4 min long. It is named after Maximilian Schuler (Pitman, 1962). In 1923, Schuler published a paper regarding the properties of a mechanical system (the specific example was a gyrocompass) tuned to maintain a local-level/locally vertical frame of reference regardless of external applied forces. Schuler's work was later shown to apply to INSs since they also implement a local-level/locally vertical frame of reference (e.g., the n-frame).

As the simulation goes on, errors start to build up in the east–west direction. This cross-coupling results from incorrect application of Earth rate (which results from an erroneous computation of latitude) in the n-frame update. If the simulation is extended, the magnitudes (i.e., envelope) of the east–west and north–south errors will slowly oscillate with a period that is inversely proportional to the sine of the latitude (Titterton and Weston, 2005). This is known as the Foucault oscillation.

1.9.6.2 Horizontal Gyroscope Bias Simulation

In this example a 0.01°/h bias is simulated on the body y-axis gyroscope. Since the vehicle is level and pointed north, the gyro is sensitive in the east direction (Figures 1.5 and 1.6).

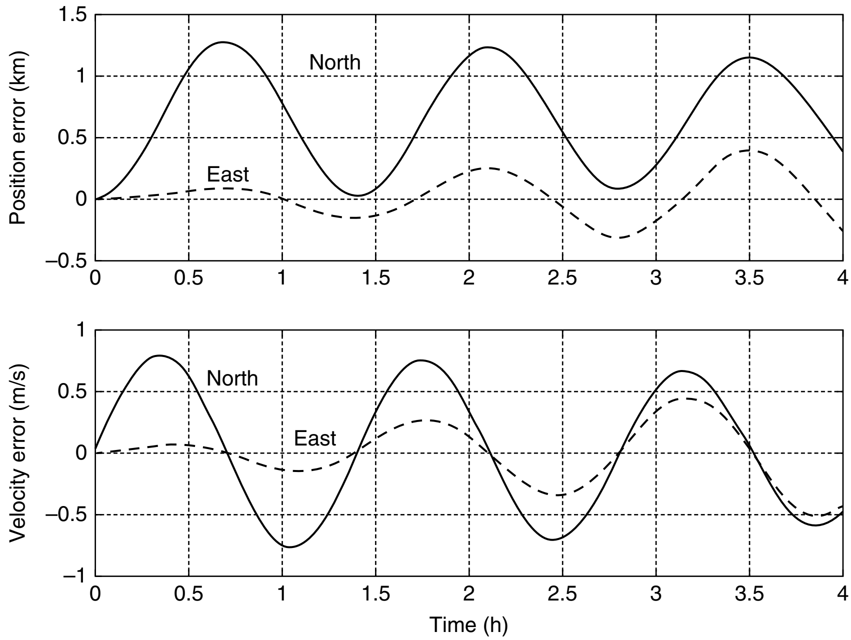

Figure 1.3 Position/velocity errors resulting from a 100 μg north accelerometer bias

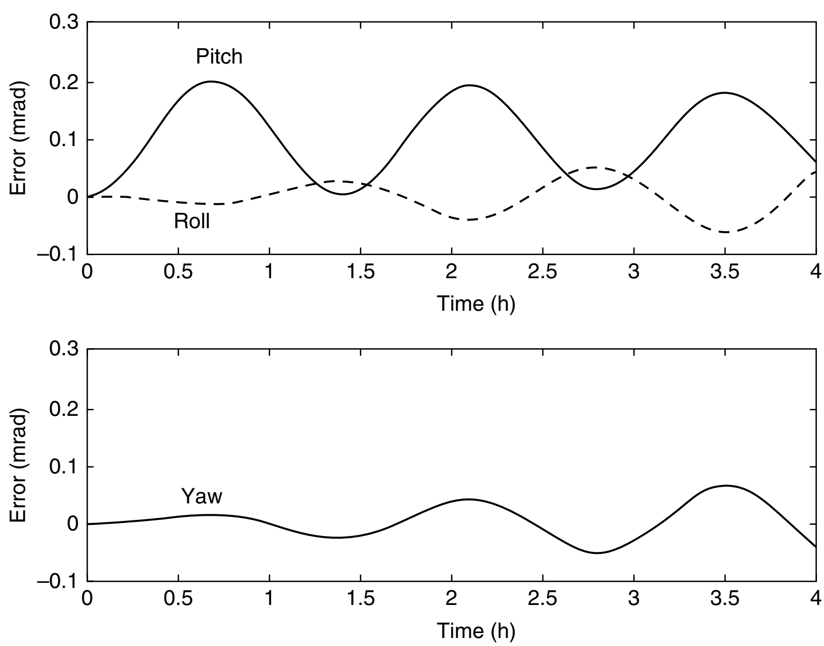

Figure 1.4 Euler angle errors resulting from a 100 μg north accelerometer bias

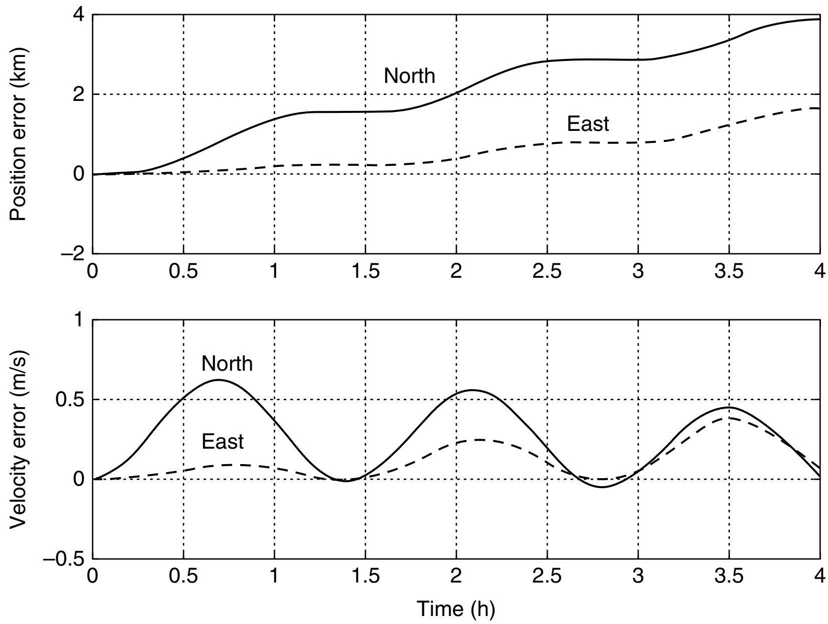

Figure 1.5 Position/velocity errors resulting from a 0.01°/h east gyroscope bias

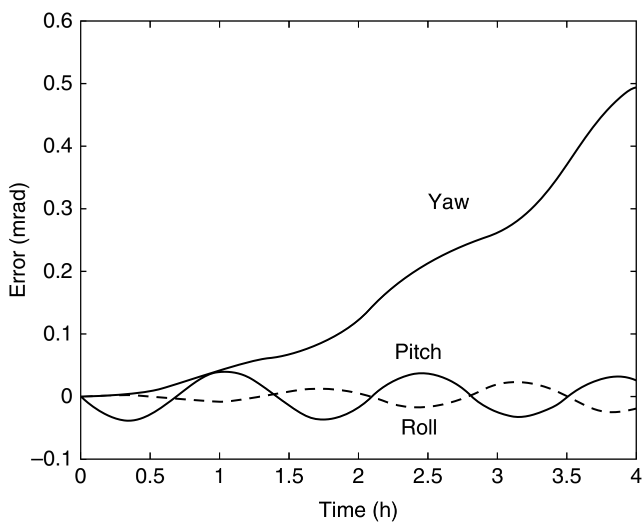

Figure 1.6 Euler angle errors resulting from a 0.01°/h east gyroscope bias

In this case, the Schuler periodicity is still present in the position error, but the dominant effect is a longer-term growth trend that is approximately linear over the first few hours. Although somewhat counterintuitive, the horizontal gyro bias induces a longer-term error growth trend in the yaw angle, whereas the bounded Schuler oscillations are present in the roll and pitch angles.

1.9.6.3 Vertical Gyroscope Bias Simulation

In this example, a 0.01°/h bias is simulated on the body z-axis gyroscope. Since the vehicle is level, the gyro is sensitive to yaw motion in the vertical direction (Figures 1.7 and 1.8).

In this case, the linear error growth trend is observed on the velocity components, and the position error growth is then quadratic. Nevertheless, the position error growth is still slower for the vertical gyro bias than was the case for the horizontal gyro bias.

1.9.6.4 Azimuth Initialization Error Simulation

In this example, a 1 mrad error in the initial azimuth (yaw) determination is simulated (Figures 1.9 and 1.10).

It is noted that the position, velocity, and attitude error characteristics for an initial azimuth error are very similar to those for a horizontal gyro bias.

1.9.6.5 Velocity Initialization Error Simulation

In this example, a 0.1 m/s error in the initial north velocity determination is simulated (Figures 1.11 and 1.12).

Virtually pure Schuler oscillations are present, and it is noted that all the errors in this case are zero mean over the long term. The magnitudes of the errors scale with the magnitude of the initial velocity error. An initial velocity error of 1 m/s would therefore result in a peak position error of approximately 0.8 km.

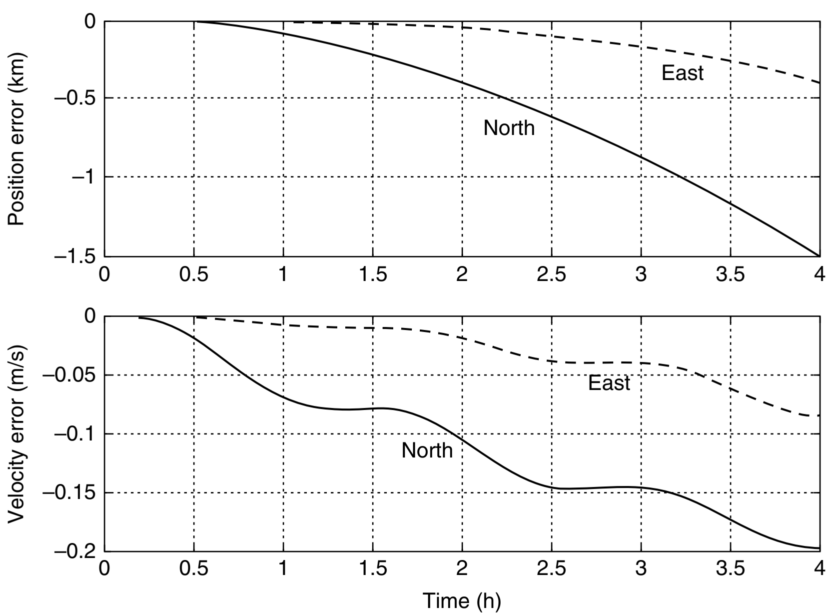

Figure 1.7 Position/velocity errors resulting from a 0.01°/h vertical gyroscope bias

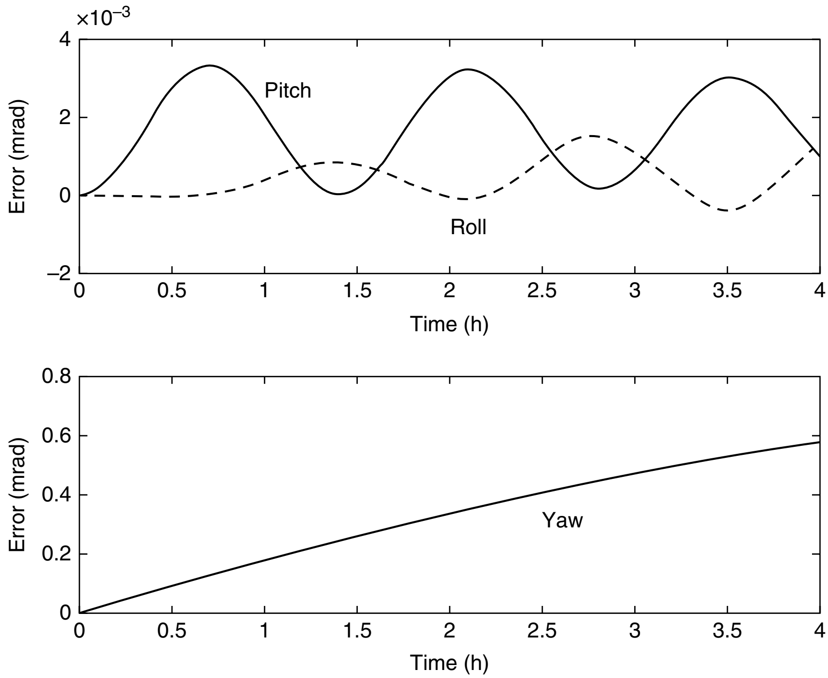

Figure 1.8 Euler angle errors resulting from a 0.01°/h vertical gyroscope bias

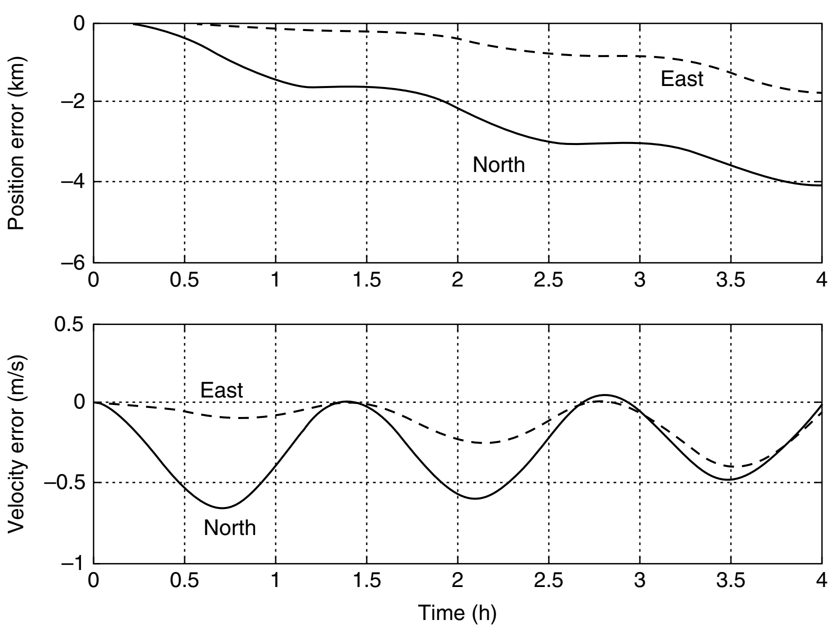

Figure 1.9 Position/velocity errors resulting from a 1 mrad initial azimuth error